crystals

MDPI

Article

Thickness Debit Effect in Creep Performance of a Ni_3Al-Based Single-Crystal Superalloy with [001] Orientation

Shuangqi Zhang [1], Guoquan Ma [1], Haibo Wang [2], Wenqi Guo [3], Haigen Zhao [3], Yong Shang [2], Yanling Pei [2], Shusuo Li [3,4,*] and Shengkai Gong [2,4]

1 School of Materials Science and Engineering, Beihang University, Beijing 100191, China
2 Frontier Research Institute of Innovative Science and Technology, Beihang University, Beijing 100191, China
3 Research Institute of Aero-Engine, Beihang University, Beijing 100191, China
4 AECC Guizhou Liyang Aviation Power Company Limited, Guiyang 550014, China
* Correspondence: lishs@buaa.edu.cn

Abstract: With the complexity of the structure of aero-engine turbine blades, the blade wall thickness continues to decrease. It is found that when the blade wall thickness decreases to a certain extent, its mechanical properties will decline significantly. It is extremely important to study this phenomenon of a significant decline in mechanical properties caused by wall thickness. In this paper, the creep behavior of a second-generation Ni_3Al-based single crystal superalloy with different wall thicknesses and [001] orientation at 980 °C/220 MPa has been studied and compared with the creep life of Φ4 round bar. The experimental results show that the second orientation and the surface affected zone are not the main reasons for the reduction of the life of thin-walled samples under this experimental condition. By analyzing the fracture morphology and deformed microstructure of thin-walled samples with different thicknesses, it is found that the thickness debit effect of the single crystal alloy occurs since the effective stress area of the alloy changes due to internal defects and surface affected zone during the creep process. For thicker samples, the creep life of the alloy can be extended by making the samples undergo certain plastic deformation through better plastic deformation coordination ability, while for thinner samples, the plastic coordination ability is poor, and the ability to extend the creep life through plastic deformation is also weaker when the effective stress area of the alloy changes, which leads to the thinner samples being more prone to fracture.

Keywords: single crystal; thickness debit effect; creep; Ni_3Al-based superalloys

check for updates

Citation: Zhang, S.; Ma, G.; Wang, H.; Guo, W.; Zhao, H.; Shang, Y.; Pei, Y.; Li, S.; Gong, S. Thickness Debit Effect in Creep Performance of a Ni_3Al-Based Single-Crystal Superalloy with [001] Orientation. *Crystals* **2023**, *13*, 200. https://doi.org/10.3390/cryst13020200

Academic Editors: Pavel Lukáč, Ronghai Wu and Xiaoxiang Wu

Received: 4 January 2023
Revised: 19 January 2023
Accepted: 21 January 2023
Published: 22 January 2023

Copyright: © 2023 by the authors. Licensee MDPI, Basel, Switzerland. This article is an open access article distributed under the terms and conditions of the Creative Commons Attribution (CC BY) license (https://creativecommons.org/licenses/by/4.0/).

1. Introduction

As an intermetallic compound phase, Ni_3Al has a high specific strength and specific stiffness, especially good high-temperature mechanical properties. Ni_3Al phase contains high Al content, which has a low density compared with other alloy elements. Therefore, Ni_3Al-based single-crystal superalloys also have the advantage of low density. Ni_3Al-based single crystal superalloy mainly consists of γ and γ' phases. Under the condition of high temperature and stress, the two phases will undergo complex changes. This change in microstructure will affect the mechanical properties of the material. Therefore, it is very important to study Ni_3Al-based single crystal superalloy [1–4].

Because of the excellent properties of Ni_3Al-based single-crystal superalloy, it has attracted extensive attention as a candidate material for aero-engine turbine blades. In recent years, researchers have paid attention to the lightweight of turbine blades to meet the increasing design requirements of aero-engine turbine blades [5]. To make the blade lighter and thinner, researchers have continuously reduced the section size of specific parts of the blade and found that when the section size is reduced to a certain extent, the mechanical properties of these parts will decline significantly, which seriously affects the performance of the aero-engine. Therefore, people began to study the reason for

performance degeneration caused by the change in section size [1,6–8]. The thickness debit effect is also called the section size effect, which means that when the size of the section direction of the part decreases to a certain extent, its mechanical properties will change significantly compared with the standard test bar [9,10].

The thickness debit effect of single crystal superalloys has been studied by researchers [11–16]. Some researchers believe that the thickness debit effect of single-crystal alloys is mainly caused by surface oxidation behavior [17,18]. Brunner et al. believed that the thin-walled sample has a high proportion of surface area, resulting in its performance being greatly affected by surface changes [19]. It is obvious that oxidation will be affected by the surface state of the alloy, such as secondary orientation. Zhao studied the relationship between the second orientation and the properties of thin wall samples of DD6 single crystal superalloy at 850 °C/560 MPa and 980 °C/250 MPa. It was found that when the primary orientation was [001], the greater the deviation of the second orientation from the [010] direction, the more the creep properties decreased [7,20]. At present, there are many kinds of research on the effects of primary orientation on the properties of tubes, but there is a lack of research on the effects of different secondary orientations on the properties of thin walls.

At present, studies on the thickness debit effect of single-crystal superalloys mainly focus on Ni-based single-crystal alloys, and no uniform explanation has been provided for the cause of the thickness debit effect. Furthermore, studies on the thickness debit effect of Ni_3Al-based single crystal alloys are even fewer [7,21]. Therefore, based on a second-generation Ni_3Al-based single crystal superalloy, the creep life of the alloy with three kinds of wall thickness samples of 0.3, 0.5, and 0.7 mm at 980 °C/220 MPa was studied in this paper. By comparing the creep life with that of Φ4 round bar, whether the three samples will produce the thickness debit effect is analyzed. The main influencing factors of the thickness debit effect of the alloy are revealed by analyzing the microstructure, which will provide some references for the subsequent research on the thickness debit effect.

2. Experimental

The alloy used in the test was a second-generation Ni_3Al-based single-crystal superalloy. After being refined at about 1600 °C in a directional solidification furnace, it was cast into the mold shell. Then the mold shell was pulled out of the insulation area at a speed of 4.5 mm/min, and the single crystal test bar was obtained by removing the mold shell after cooling. The single crystal test bar was etched with hydrochloric acid hydrogen peroxide solution to check the integrity of the single crystal. The main essential components are listed in Table 1. Test bars with good single crystal integrity for standard heat treatment (1300 °C, 2 h/1310 °C, 2 h/1320 °C, 2 h/1325 °C, 4 h/1330 °C, 6 h/argon gas cooling/1040 °C, 6 h/argon gas cooling/870 °C, 6h/furnace cooling) were selected.

Table 1. Composition of the used Ni_3Al-based single-crystal superalloy (mass %).

Element	Ni	Al	Cr	Mo	Re	Ta	Y
Content	Excess	7.6–8.3	1.5–2.5	9–13	0.5–1.5	2.4–4.0	0.01

The X-ray backscattering Laue method was used to conduct the crystal orientation test along the axis of the test bar. The test bar with the primary orientation deviating less than 5 ° from the [001] direction was selected. With the consideration of the secondary orientation, the secondary orientation perpendicular to the side of the sample was controlled to deviate less than 5 ° from the [110] and [010] directions, respectively. The specific sampling method and sample size are shown in Figures 1 and 2.

In order to ensure the surface quality of the thin wall sample, the 1 mm thick sample was processed by wire cutting, and then the surface and side of the sample were ground with 400, 600, 800, 1000, 1200, and 1500 silicon carbide sandpaper in turn. The error in the thickness direction of the sample was ±0.02 mm. Finally, the surface of the sample was polished with a diamond polish of 0.5 nm particles. The surface of the treated sample was required to be free of obvious scratches and other defects.

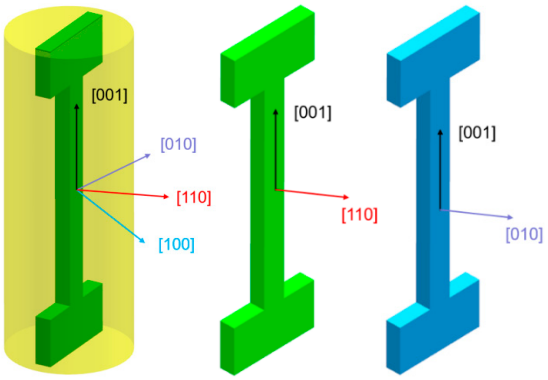


Figure 1. The schematic of samples with [001] primary orientation and different secondary orientation with [110] and [010].

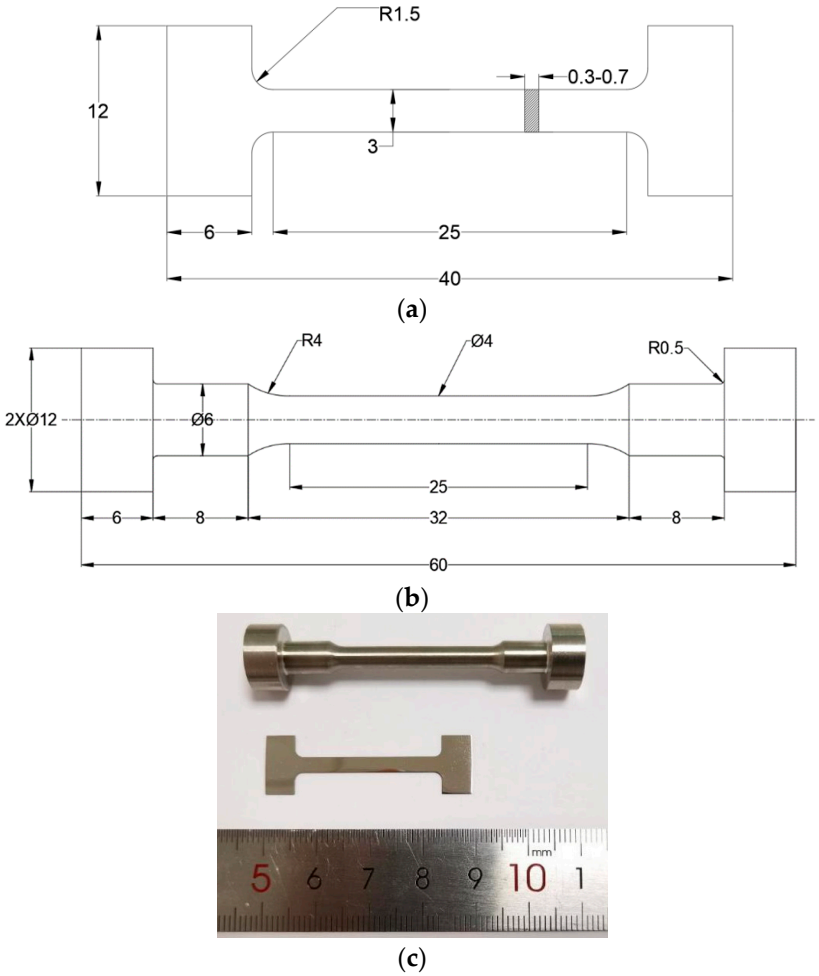


Figure 2. Test pieces' sizes: (**a**) Thin wall sample size, (**b**) Φ4 round bar size, (**c**) picture of the sample.

All creep tests were conducted according to the uniaxial tensile creep test method for metallic materials (GB/T 2039-2012), and the test conditions were 980 °C/220 MPa. After the test, samples were taken from the fracture area and test section of the sample, respectively, for polishing. The reagent prepared by CuSO4+100mL HCl+100mL C2H5OH was used for corrosion. All the microstructure characterizations were conducted by scanning electron microscope (SEM, Apreo S LoVac, FEI, Czech) equipped with an electron backscatter diffraction (EBSD) system (orientation analysis) operated at 25 kV and an energy dispersive spectroscopy (EDS) system operated at 20 kV. The fracture surface of the

sample was treated by ultrasonic cleaning, the fracture morphology and microstructure were observed by SEM, and the surface oxide composition was analyzed by EDS. To further analyze the crystal change, EBSD was used to characterize the crystal rotation near the fracture surface of the sample.

3. Results and Discussion

In order to study the influence of wall thickness and secondary orientation on the creep property of the sample, thin wall samples with the second orientation of [110] and [010] are selected for testing. The creep life of thin wall samples with different thicknesses and Φ4 samples is shown in Figure 3.

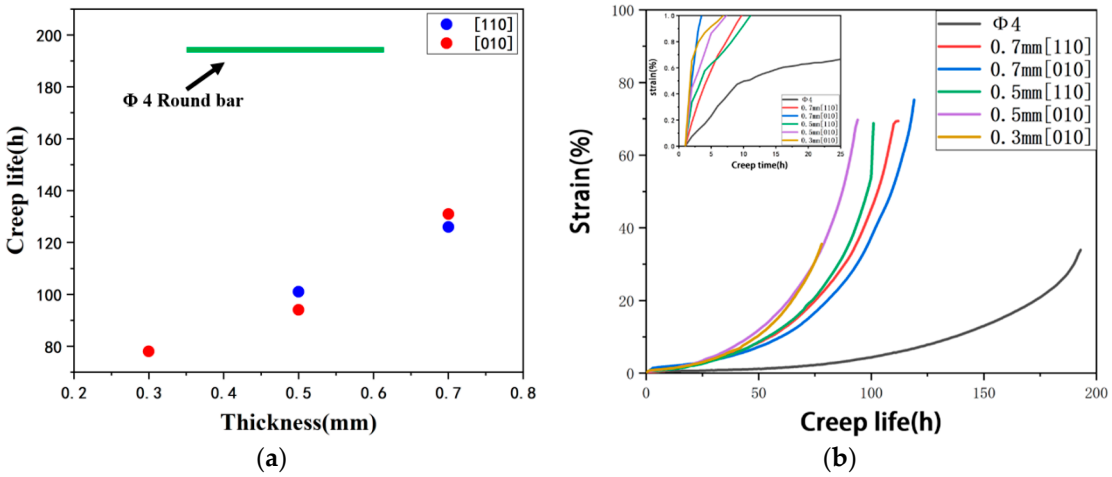


Figure 3. Creep life of thin-walled samples with different thicknesses and Φ4 round bar samples at 980 °C/220 MPa. (**a**) Relationship between wall thickness and creep life. (**b**) The creep curves at 980 °C/220 MPa.

It can be seen from Figure 3a that the creep life of the 0.3–0.7 mm thin-walled sample is far less than Φ4 round bar sample. The creep life of the thin wall sample with a wall thickness of 0.7 mm is 38% lower than that of the Φ4 round bar sample. The creep life of the 0.5 mm thin wall sample is 48% lower than that of the Φ4 round bar sample. The creep life of 0.3 mm thin wall sample is 60% lower than that of the Φ4 round bar sample. Since the creep life has decreased by 38% at 0.7 mm, which is much smaller than that of the Φ4 round bar sample, it can be determined that the Ni_3Al-based single crystal superalloy has produced the thickness debit effect when the wall thickness is smaller than 0.7 mm. At the same time, there is little difference between the creep life of the thin-walled sample with the second orientation of [110] and [010], that is, the secondary orientation has no obvious effect on the creep life of the thin-walled sample under this test condition. It can be seen from Figure 3b that the strain of the Φ4 round bar sample is about 34%, while the average strain of 0.5 and 0.7 mm thin-walled sample is about 69%, and the strain of 0.3 mm thin-walled sample is about 36%. It can be seen from the strain that when the thickness debit effect is produced, the strain will also decrease significantly when the wall thickness reaches a certain value. Thin-walled samples take much shorter periods of 1% strain than round-bar samples. It can also be seen from the figure that the thin-walled sample has no obvious second stage of creep, and its strain and strain rate increase with time until the sample breaks.

Figure 4 is the fractured image of the sample with primary orientation [001] and secondary orientation [010]. It can be seen from Figure 4a–c that the fracture surfaces of 0.3–0.7 mm thin wall samples are rectangular, and the thickness of the fracture surfaces are 0.23, 0.32, and 0.48 mm, respectively. The height difference between the left and right sides of the fracture surface is very small, and there are dimples inside. The fracture surface of the standard round bar sample is basically circular, and the diameter changed from Φ4 to

Φ3.4. The interior is full of tearing edges. It can be seen from the fracture surface of the thin-walled sample that the fracture surface thickness of the 0.3 mm sample decreases by 23%, and the average fracture surface thickness of the 0.5 and 0.7 mm samples decreases by 33.5%. Therefore, the deformation of the 0.3 mm sample in the length and thickness direction is smaller than that of the other two thickness samples, the differences regarding deformation are revealed in the following discussion part.

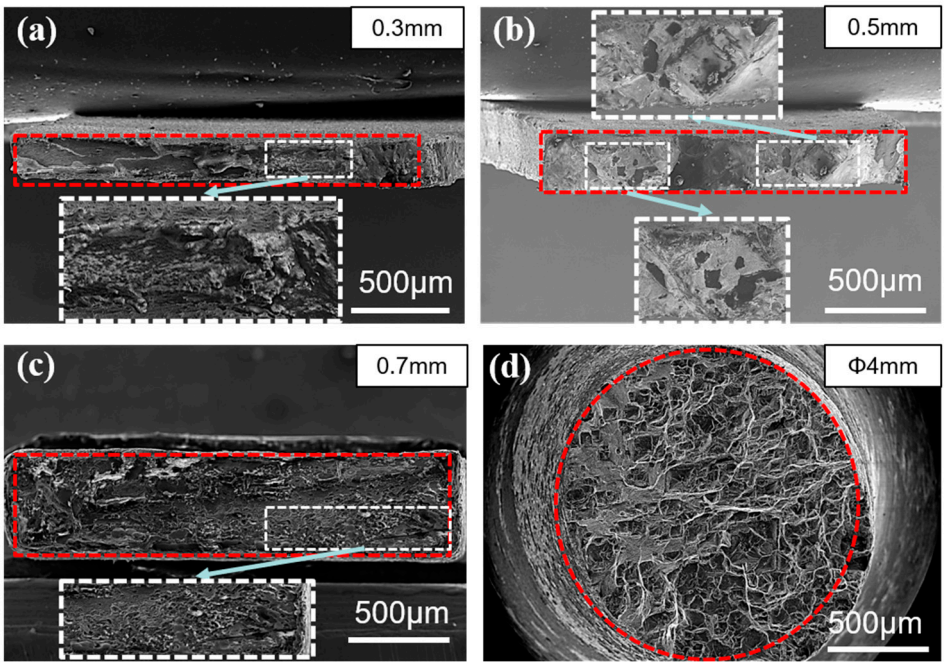


Figure 4. Thin-walled samples with different thicknesses and Φ4 round bar at 980 °C/220MP fracture of sample (**a**) fracture surface of 0.3 mm sample, (**b**) fracture surface of 0.5 mm sample, (**c**) fracture surface of 0.7 mm sample, (**d**) fracture surface of Φ4 round bar.

The white box in Figure 4a is an obvious dimple area by observing the fracture surface characteristics, while a large area of cleavage surface appears on the left side. Therefore, it is speculated that the crack will initiate and expand from the right side. When the crack expands to the left side, the sample will break instantaneously due to the smaller load-bearing area. In Figure 4b, a square cleavage surface is found in the white boxes on the left and right sides with tear edges around it, while the middle of the sample is a transient fracture zone with cleavage characteristics. A small dimple area is found in the white box in Figure 4c, and there is an obvious strip-like transient fracture area in the middle of the fracture. In Figure 4d tearing edges are distributed evenly at the fracture surface, and some cleavage surfaces are found on the left side of the fracture surface. Compared with Figure 4a, the proportion of cleavage surface in Figure 4d is far less than that in Figure 4a, indicating that the instantaneous fracture zone in the round bar sample is smaller than that in the thin wall sample. It can be seen from the analysis in Figure 4 that the three wall thickness samples all show the characteristics of mixed ductile-brittle fracture, of which the 0.3 mm thick sample has the largest transient fracture zone, indicating that the sample is more prone to fracture when the effective stress area changes in this thickness.

Figure 5 shows the composition and thickness comparison diagram of the affected zone of the sample test section, and the affected zone is the average value of the test section. It can be seen from Figure 5a that the affected zone of the alloy thin wall sample consists of the NiO zone, Al and Ni oxides zone, and γ'- free zone. Figure 5b shows the thickness of the affected zone in the test section of the thin-walled sample and the Φ4 round bar sample with the second orientation of [010]. It can be seen that the thickness of the affected zone of the Φ4 round bar sample is larger, about twice that of the thin-walled sample,

but its overall proportion in the diameter direction is only 0.94%, far less than that of the thin-walled sample. The thickness of the affected zone of 0.3–0.7 mm thick, thin-walled samples has little difference, and the proportion in the thickness direction is 3.4–7.2%. Creep experiments found that the creep life of the 0.3 mm thick sample is about 70% of that of the 0.7 mm thick sample, but the thickness of the affected zone is not much different, so the thickness of the affected zone is not the main reason for the difference in the creep life of the two thin-walled samples.

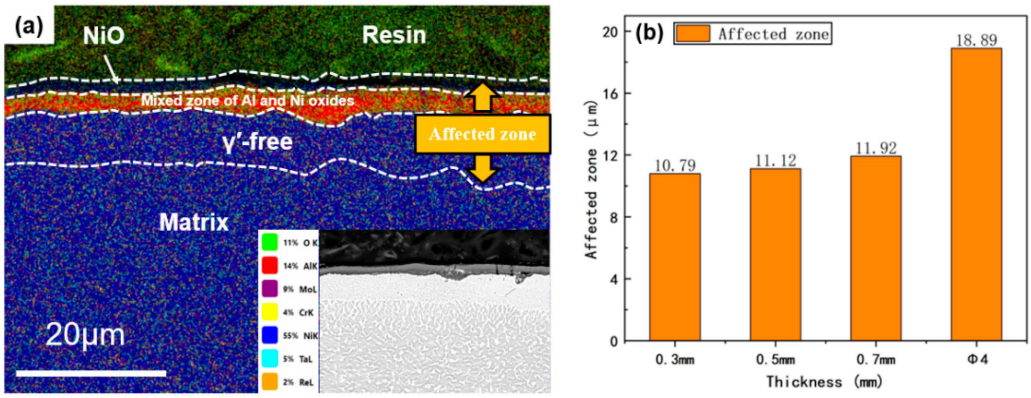


Figure 5. Thickness of affected zone in the test section of thin wall sample and Φ4 round bar sample with the secondary orientation of [010] (**a**) composition of the affected area, (**b**) thickness comparison of the affected zone.

Figure 6 shows the comparison of the affected zone in the test section of 0.7 mm thick samples with different secondary orientations. It can be seen from the figure that the thickness difference of the affected zone of the two thin-walled samples is not obvious, indicating that the second orientation of the sample in this experiment has no significant influence on the thickness of the affected zone.

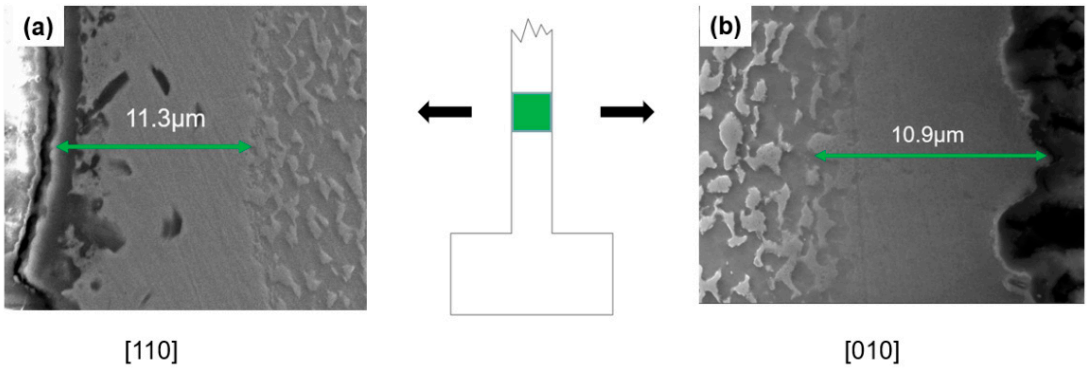


Figure 6. Thickness of affected zone of 0.7 mm thin walls (**a**) with the second orientation of [110], (**b**) with the second orientation of [010].

The microstructure comparison of the thin wall sample at 1 mm from the fracture surface is shown in Figure 7. It can be seen from the figure that the fracture microstructure of the 0.3–0.7 mm thin-walled samples presents a fine γ phase, and γ phase of 0.3 mm and 0.5 mm samples is smaller than that of 0.7 mm samples. This kind of fine γ phase is surrounded by γ′ phase, forming many "islands", that is, "Topology inversion" [22]. In the evolution of γ/γ′ phase morphology, the volume fraction of γ′ raft changes [23]. The γ′ phase is the main strengthening phase in single crystal superalloy, which is beneficial to the mechanical properties of the alloy at high temperatures, and the broken γ phase will form more γ/γ′ two-phase interfaces [24]. The γ/γ′ two-phase interface is conducive to forming

an interfacial dislocation network, which effectively hinders the dislocation movement and improves the mechanical properties of the alloy [25].

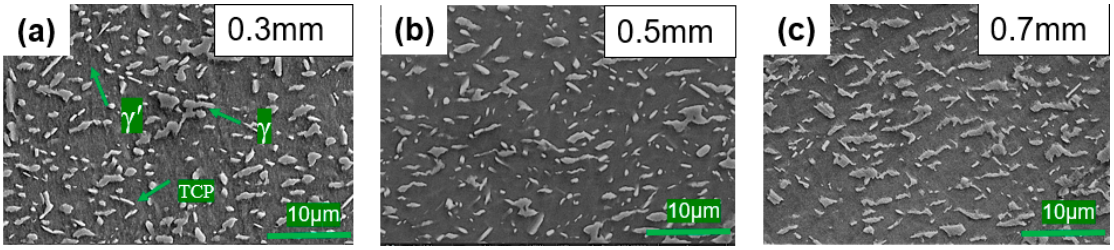


Figure 7. Microstructure of thin wall sample 1 mm from the fracture surface (**a**) 0.3 mm sample, (**b**) 0.5 mm sample, (**c**) 0.7 mm sample.

The same as in other tests, it was found in this experiment that the maximum strain variable of thin-walled samples would increase with the increase in wall thickness [8,16]. From the perspective of maximum strain, the 0.7 mm sample has a longer creep life than the 0.3 mm sample may be due to its stronger deformation coordination ability. When the plastic strain of the alloy increases due to defects such as micro holes during the creep process of the sample, the thicker sample can extend the life of the sample through stronger deformation coordination ability, while the thinner sample is difficult to extend the creep life of the sample through deformation due to poor deformation coordination ability, so it will fracture when the alloy plastic strain is large, which is also consistent with the test results of the 0.3 mm sample with deformation of less than 0.7 mm sample mentioned above. At the same time, this is consistent with the study of Huttner et al., that the creep fracture strain and creep life decrease with the decrease of the wall thickness of the sample 1–0.3 mm [26].

To verify this prediction, we analyzed the crystal rotation from the misorientation. EBSD was used to observe the misorientation at 1 mm of the fracture of 0.3 and 0.7 mm samples. The direction was parallel to the loading direction of the samples, and the length was about 650 μm. As can be seen from Figure 8a, the maximum misorientation of the 0.3 mm sample in the Z direction is 2.08°. From Figure 8b, the maximum misorientation of the 0.7 mm sample in the Z direction is 2.9°, that is, the thick sample has a greater degree of misorientation in the Z direction, and the thin sample has a smaller misorientation at fracture. This is consistent with the above results, the thinner the sample, the smaller the plastic deformation.

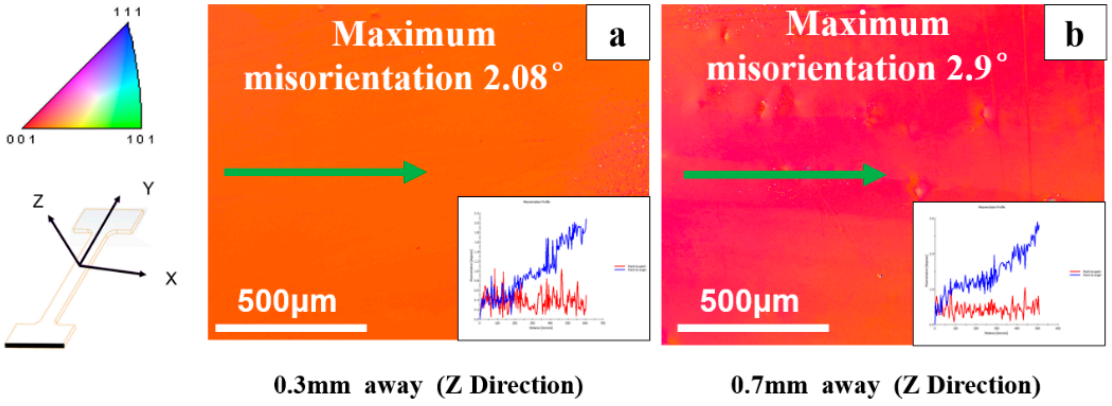


Figure 8. EBSD inverse pole figure of 0.3 and 0.7 mm sample 1 mm away from the fracture surface (**a**) Z direction of 0.3 mm sample, (**b**) Z direction of 0.7 mm sample.

From the above research, it can be seen that the second orientation has little effect on the creep life of the alloy sample with a wall thickness of 0.3–0.7 mm. The thickness

of the affected zone of the samples with different wall thicknesses is similar, and there is no significant difference, which indicates that the affected zone is not the main reason for affecting the creep life of the alloy. Through the analysis of the morphology, deformation, and microstructure of the fracture surface of the thin-walled sample, it can be inferred that the causes of the thickness debit effect of the single crystal alloy thin-walled sample are as follows: during the creep process, due to internal defects and surface affected zone, the effective force area of the alloy changes. According to Wen [27], the necking degree of thin-walled specimens increases with the increase of wall thickness at high temperatures. Combined with the above research on the wall thickness change at the fracture, the increase of necking degree is equivalent to plastic deformation, for thicker samples, plastic deformation can be made to prolong the creep life of the alloy by better plastic deformation coordination ability, but the plastic coordination ability of thinner samples is poor. When the effective force area of the alloy changes, the way of prolonging the creep life by plastic deformation is weaker, and the plastic deformation sample of the after-creep fracture is smaller. The relationship between the thickness debit effect and deformation coordination ability has been studied by researchers. We know that the plastic deformation of the alloy is closely related to its activated slip system. Lv et al. [21] studied the thickness debit effect from the slip systems, they believed that the six slip systems of the {111}<110>type and one slip system of the {111}<112>type were activated during the creep of the thin wall sample. The eight slip systems of {111}<110>type and the two slip systems of {111}<112>type of the thick sample were activated. Due to the different activated numbers of slip systems, the deformation coordination ability of thin samples is poor, which is consistent with the conclusion of this paper. The study of Huttner et al. [26] also shows that there is a relationship between sample thickness and strain, and the strain of samples decreases with the decrease of wall thickness, which is consistent with the poorer plastic compatibility of thinner samples in this paper.

4. Conclusions

In this study, the thickness debit effect in creep performance of a Ni_3Al-based single crystal superalloy was studied. Through comparative analysis of sample orientation, affected zone, and microstructure, the following main conclusions are obtained:

1. The Ni_3Al-based single crystal superalloy studied in this experiment has an obvious thickness debit effect for 0.3–0.7 mm samples at 980 °C/220 MPa. It is found through the test that the second orientation [110] and [010] have no significant effect on the creep life of the thin wall samples.

2. By comparing the thickness of the affected zone of the sample with 0.3–0.7 mm thin wall, it is found that the thickness difference of the affected zone of the samples is not significant, indicating that the affected zone is not the main reason for the reduced life of the sample with a thin wall.

3. Based on the analysis of the microstructure of the thin-walled sample and the plastic deformation of the sample after fracture, a possible cause of the thickness debit effect was proposed. The thicker sample has better deformation coordination ability than the thinner one. When the stress condition of the sample changes due to defects in the creep process, the thicker sample can produce plastic deformation through its better deformation coordination ability and thus prolong the creep life, but the thinner sample can only prolong the creep life with smaller plastic deformation amount due to its poor deformation coordination ability. As a result, its creep life is shorter, and its fracture strain is smaller.

Author Contributions: Conceptualization, S.L. and S.G.; methodology, W.G.; formal analysis, Y.S.; investigation, H.Z. and Y.P.; data curation, H.W.; writing—original draft preparation, S.Z.; writing—review and editing, G.M. All authors have read and agreed to the published version of the manuscript.

Funding: This paper is supported by Science Center for Gas Turbine Project (NO. P2021-A-IV-001-003), National Natural Science Foundation (NO. 52103358), and National Science and Technology Major Project (2017-VI-0012-0084), Science Center for Gas Turbine Project (NO. P2022-B-IV-009-001).

Data Availability Statement: The data presented in this study are available on request from the corresponding author. The data are not publicly available due to [Alloy material sensitivity problem].

Conflicts of Interest: The authors declare no conflict of interest.

References

1. Xiong, W.; Ai, X.; Wang, J.; Wang, Q.; Zhao, Y.; Zhu, H.; Cheng, H.; Zhang, S. Study of the Creep Behavior of Nickel-Based Single Crystal Superalloy Micro Samples with Dimensional Effects. *Crystals* **2022**, *12*, 592. [CrossRef]
2. Chen, Y.; Zhang, W.; Zhao, Y.; Zhai, Y.; Zhang, B.; Lu, H.; Yang, G.; Yang, L.; Li, A. Oxidation-induced rhenium evaporation in Ni-based single crystal superalloy thin lamella. *Scr. Mater.* **2021**, *203*, 114106. [CrossRef]
3. He, X.; Zhang, J.; Peng, Y.; Li, J.; Ding, J.; Liu, C.; Xia, X.; Chen, X.; Liu, Y. Microstructure Evolution of Primary γ′ Phase in Ni_3Al Based Superalloy. *Acta Metall. Sin.* **2020**, *33*, 1709–1726. [CrossRef]
4. Jiang, L.; Yang, Y.; Wu, M.; Cai, M. Anisotropy Study on Creep Behavior of a Ni_3Al Based Single Crystal Superalloy at 1100 °C/137 MPa. *Rare Met.* **2021**, *45*, 1025–1033.
5. Liu, W.; Zhu, O. Study on Thin Wall Effect of Single Crystal Blade for Aeroengine. *Cast. Technol.* **2017**, *38*, 2571–2575.
6. Hüttner, R.; Gabel, J.; Glatzel, U.; Völkl, R. First creep results on thin-walled single-crystal superalloys. *Mater. Sci. Eng. A* **2009**, *510–511*, 307–311. [CrossRef]
7. Hu, Y.; Zhang, L.; Cheng, C.; Zhao, P.; Cao, T.; Guo, G.; Zhao, J. Influence of sample thickness on the creep behavior of a directional solidification nickel-based superalloy. *Vacuum* **2018**, *150*, 105–115. [CrossRef]
8. Hu, Y.; Zhang, L.; Cao, T.; Cheng, C.; Zhao, P.; Guo, G.; Zhao, J. The effect of thickness on the creep properties of a single-crystal nickel-based superalloy. *Mater. Sci. Eng. A* **2018**, *728*, 124–132. [CrossRef]
9. Zheng, Y. Size effect of a thin section of single crystal turbine blade alloy. *Mater. Eng.* **2007**, *7*, 74–77.
10. Yu, Z.Y.; Wang, X.M.; Liang, H.; Li, Z.X.; Li, L.; Yue, Z.F. Thickness debit effect in Ni-based single crystal superalloys at different stress levels. *Int. J. Mech. Sci.* **2020**, *170*, 105357. [CrossRef]
11. Li, Y. *Creep Anisotropy of a Third Generation Nickel Base Superalloy*; University of Science and Technology of China: Hefei, China, 2019.
12. Li, Q. *Analysis of the Relationship between High Temperature Rupture Strength and Wall Thickness Effect of DD6 Alloy*; Dalian University of Technology: Dalian, China, 2016.
13. Yu, C.; Yu, J.; Yu, F.; Shi, F.; Sun, F. Thin wall effect on stress rupture properties of DD499 single crystal alloy. *Casting* **2014**, *63*, 479–483.
14. Fourie, J.; Baldan, A. *Size Effects in the Mechanical Properties of Superalloy Single Crystals*; TMS: Philadelphia, PA, USA, 1992.
15. Wen, Z.; Liang, J.; Liu, C.; Pei, H.; Wen, S.; Yue, Z. Prediction method for creep life of thin-wall sample with film cooling holes in Ni-based single-crystal superalloy. *Int. J. Mech. Sci.* **2018**, *141*, 276–289. [CrossRef]
16. Brice, C.; Alexander, S. The effect of thickness on the creep response of thin-wall single crystal components. *Mater. Sci. Eng. A* **2008**, *508*, 183–189.
17. Zhang, L.; Yu, H.; Guo, G.; Zhao, J.; Zhao, P. Stress rupture properties and fracture behavior of thin-walled samples of oriented DD6 single crystal alloy. *J. Aerodyn.* **2019**, *34*, 627–634.
18. Srivastava, A.; Gopagoni, S.; Needleman, A.; Seetharaman, V.; Staroselsky, A.; Banerjee, R. Effect of sample thickness on the creep response of a Ni-based single-crystal superalloy. *Acta Mater.* **2012**, *60*, 5697–5711. [CrossRef]
19. Brunner, M.; Bensch, M.; Völkl, R.; Affeldt, E.; Glatzel, U. Thickness influence on creep properties for Ni-based superalloy M247LC SX. Materials science & engineering. *Struct. Mater. Prop. Microstruct. Process.* **2012**, *550*, 254–262.
20. Zhao, J. Effect of secondary orientation on the rupture properties of single crystal superalloy DD6. In Proceedings of the China Materials Conference 2021, Xiamen, China, 9 July 2021. Available online: https://kns.cnki.net/kcms/detail/detail.aspx?FileName=ZGCZ202107001041&DbName=CPFD2021 (accessed on 3 January 2023).
21. Lv, J.; Zhao, Y.; Wang, S.; Zhao, X.; Zhao, J.; Zheng, L.; Guo, Y.; Schmitz, G.; Ge, B. Stress state mechanism of thickness debit effect in creep performances of a Ni-based single crystal superalloy. *Int. J. Plast.* **2022**, *159*, 103470. [CrossRef]
22. Ru, Y.; Hu, B.; Zhao, W.; Zhang, H.; Pei, Y.; Li, S.; Gong, S.; Xu, H. Topologically inverse microstructure in single-crystal superalloys: Microstructural stability and properties at ultrahigh temperature. *Mater. Res. Lett.* **2021**, *9*, 497–506. [CrossRef]
23. Murakumo, T.; Kobayashi, T.; Koizumi, Y.; Harada, H. Creep behaviour of Ni-base single-crystal superalloys with various gamma' volume fraction. *Acta Mater.* **2004**, *52*, 3737–3744. [CrossRef]

24. Chen, J.; Cao, L.; Tang, X.; Xue, M. A kind of Ni_Microstructure and high plastic deformation behavior of 3Al based single crystal superalloy. *J. Mater. Heat Treat.* **2016**, *37*, 33–37.
25. Li, Y.; Wang, L.; He, Y.; Zheng, W.; Lou, L.; Zhang, J. Role of interfacial dislocation networks during secondary creep at elevated temperatures in a single crystal Ni-based superalloy. *Scr. Mater.* **2022**, *217*, 114769. [CrossRef]
26. Hüttner, R.; Völkl, R.; Gabel, J.; Glatzel, U. Creep behavior of thick and thin walled structures of a single crystal nickel-base superalloy at high temperatures—Experimental method and results. *Superalloys* **2008**, *2008*, 719–723.
27. Wen, Z.; Pei, H.; Li, D.; Yue, Z.; Gao, J. Thickness Influence on the Creep Response of DD6 Ni-Based Single-Crystal Superalloy. *High Temp. Mater. Process.* **2016**, *35*, 871–880. [CrossRef]

Disclaimer/Publisher's Note: The statements, opinions and data contained in all publications are solely those of the individual author(s) and contributor(s) and not of MDPI and/or the editor(s). MDPI and/or the editor(s) disclaim responsibility for any injury to people or property resulting from any ideas, methods, instructions or products referred to in the content.